The adsorption of dipoles at a wall in the presence of an electric field: The RLHNC approximation[a)]

John M. Eggebrecht, Dennis J. Isbister,[b)] and Jayendran C. Rasaiah

Department of Chemistry, University of Maine, Orono, Maine 04469
(Received 12 May 1980; accepted 10 June 1980)

The adsorption of dipolar hard spheres in the presence of an external electric field has previously been studied within the context of the mean spherical approximation. In order to quantify the significance of the physical trends found above, the problem is solved within the higher order closure rules afforded by the linearized hypernetted chain approximation. Expressions for the reduced dipole moment and the electric field strength are derived using only the asymptotic forms of the direct correlation functions. It is found that the favorable orientational correlations between the dipolar hard spheres and the wall are underestimated by the mean spherical approximation. This is emphasized in the enhanced adsorption of the dipolar species (at the wall itself) for dipoles oriented close to the direction of the field. However, the nonphysical features of the mean spherical approximation (manifested in the negativity of the density profile) are not fully rectified by the use of the linearized hypernetted chain approximation.

I. INTRODUCTION

The adsorption of dipolar molecules at a wall, in the presence of an electric field, is of interest in the study of electrode and membrane phenomena. Here the adsorption phenomenon is delineated by the distribution of molecules at a particular orientation Ω_1 and distance z from a hard planar wall $\rho_1(z, \mathbf{E}_2, \Omega_1)$. The electric field $\mathbf{E}_2$ emanates from this wall, the declination of the field with respect to the wall being allowed by its nonconductive properties. Isbister and Freasier[1] have investigated this problem for hard dipolar spheres against a hard wall using the mean spherical approximation (MSA). Their results for the density profile $\rho_1(z, \mathbf{E}_2, \Omega_1)$ of dipoles are of great interest even though they suffer from the defect that the wall particle density profile $\rho_1(z, \mathbf{E}_2, \Omega_1)$ assumes negative values at certain relative orientations of electric field ($\mathbf{E}_2$) and dipole moment $\mathbf{m}_1$ of the particles in the fluid (the dipole orientation is denoted here by Ω_1). However, the argument leading to the electric field at the wall is not swayed by the approximation used, and may be employed with more accurate theories such as, for example, the linearized hypernetted chain (LHNC) approximation. While these theories could be expected to produce better results, they do suffer from the necessity of employing numerical methods to a greater extent than is needed to determine the density profiles in the mean spherical approximation.

This paper is devoted to a study of the wall–particle density profile using the linearized hypernetted chain approximation[2] for the wall particle and particle–particle interactions, except that the effects that are independent of the orientations of the electric field and the fluid dipole are treated exactly. In our study, these are the interactions between the hard cores in the fluid, and also the interactions between these cores and the hard wall. We call this the renormalized linearized hypernetted chain approximation (RLHNC) after the nomenclature introduced by Stell and Weis.[3] Our results for this theory are an improvement over the corresponding MS approximation when the system is characterized by (a) a reduced fluid density $\rho_1^* = \rho_1 R_{11}^3$ of 0.573. (b) a reduced dipole moment $m_1^* = m_1/\sqrt{kTR_{11}^3}$ of $\sqrt{0.5}$ (or equivalently a reduced temperature $T^* \equiv 1/m_1^{*2}$ of 2), and (c) a reduced external electric field $E_2^* = E_2 R_{11}^3/m_1$ of 8/3. In contrast to the MS approximation, the RLHNC wall–particle density functions $\rho_1(z, \mathbf{E}_2, \Omega_1)$ are only marginally negative near the wall for a dipole orientation in direct opposition to the field (see Fig. 2). These functions, however, can become negative over a larger distance z from the wall when the reduced dipole moment is increased to 1.0 without altering the reduced electric field or reduced density (Fig. 5). This suggests even higher order terms, beyond the RLHNC approximation, must be included in the theory when the dipole moment m_1 and the external electric field E_2 are both large.

II. GENERAL THEORY

The technique of producing a wall next to a fluid by taking the limiting behavior of a binary mixture (with densities ρ_1, ρ_2 and radii R_1, R_2) detailed by

$$\lim_{R_2 \to \infty} \lim_{\rho_2 \to 0} \tag{2.1}$$

is well known.[4] Isbister and Freasier[1] have extended this to introduce an electric field, as well, by considering the corresponding limit for a dipolar mixture under the restriction that the dipole moment m_2 of particle 2, which eventually becomes the wall, divided by the cube of the radius of the excluded volume $R_{21} = R_2 + R_1$ is a constant (hereafter called E_0):

$$\lim_{R_2 \to \infty} m_2/R_{21}^3 = E_0 \ . \tag{2.2}$$

In taking these limits, in the specific order $\rho_2 \to 0$, $R_2 \to \infty$, the volume of the system is allowed to grow faster than R_2^3, keeping ρ_1 constant through the constraint that $\rho_2 R_2^3 \to 0$.

The magnitude and direction of the electric field $\mathbf{E}_2$

[a)] Extracted in part from the M.S. (Chemistry) thesis of J. Eggebrecht, University of Maine (1980).

[b)] Present address: Department of Chemistry, Faculty of Military Studies, University of New South Wales, RMC, Duntroon, ACT 2600, Australia.

 0021-9606/80/203980-07$01.00

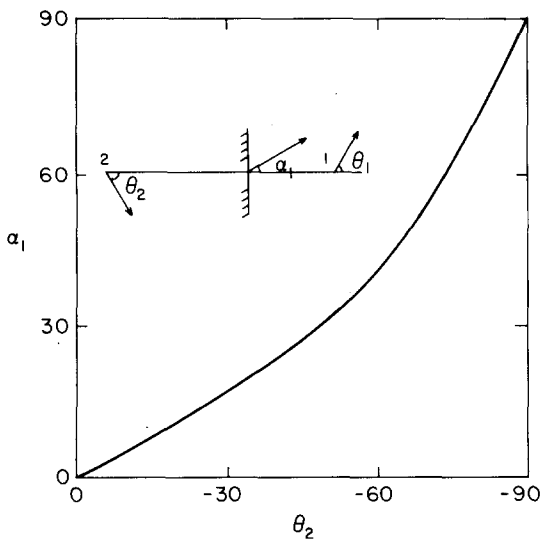

FIG. 1. The electric field angle α_1 at the wall plotted against the inclination θ_2 of the "wall dipole" which resides at minus infinity and produces the electric field E_2. The angle θ_1 is the inclination of a dipole in the bulk fluid.

follow, when this limit is applied to the dipole–dipole interaction energy

$$V_{21}(\mathbf{r}_{21}, \Omega_2, \Omega_1) = -\frac{m_1 m_2}{r_{21}^3} D(2,1) \ . \tag{2.3}$$

Here

$$D(2,1) = \hat{s}_1 \cdot (3\hat{r}_{21}\hat{r}_{21} - \mathbf{U}) \cdot s_2 \ , \tag{2.4}$$

$\hat{s}_1$ and $\hat{s}_2$ are unit vectors in the directions of the dipole moment vectors $\mathbf{m}_1$ and $\mathbf{m}_2$, respectively, $(3\hat{r}_{21}\hat{r}_{21} - \mathbf{U})$ is the dipole–dipole interaction tensor, in which $\hat{r}_{21}$ is a unit vector in the direction along the line joining particles 1 and 2, and U is the unit tensor. The potential may be written in terms of the electric field $\mathbf{E}_2$, produced at the location of particle 1 by the second particle 2,

$$V_{21}(\mathbf{r}_{21}, \Omega_2, \Omega_1) = -m_1 \hat{s}_1 \cdot \mathbf{E}_2 \ , \tag{2.5}$$

where

$$\mathbf{E}_2 = \frac{m_2}{r_{21}^3} \mathbf{e}_2 \ . \tag{2.6}$$

In Eq. (2.6)

$$\mathbf{e}_2 = (3\hat{r}_{21}\hat{r}_{21} - \mathbf{U}) \cdot \hat{s}_2 = (3\hat{r}_{21}\cos\theta_2 - \hat{s}_2) \tag{2.7}$$

and θ_2 is the angle which the dipole embedded in particle 2 makes with $\hat{r}_{21}$ (see Fig. 1). Since the magnitude of $\mathbf{e}_2$ is $(3\cos^2\theta_2 + 1)^{1/2}$,

$$\mathbf{E}_2 = \frac{m_2}{r_{21}^3} (3\cos^2\theta_2 + 1)^{1/2} \hat{e}_2 \ , \tag{2.8}$$

where $\hat{e}_2$ is a unit vector in the direction of $\mathbf{E}_2$. Changing variables to $r_{21} = R_2 + z$, and taking the wall limit, the electric field

$$\mathbf{E}_2 = E_0 (3\cos^2\theta_2 + 1)^{1/2} \hat{e}_2 \ , \tag{2.9}$$

which shows that $\mathbf{E}_2$ is independent of the distance z from the wall, but that its magnitude is determined by the strength (through E_0) and the direction (through θ_2) of the "wall dipole," which has receded to a distance $-\infty$ from the wall. At that distance, the vector $\mathbf{r}_{21}$ becomes perpendicular to the wall, and the electric field which makes an angle α_1 with respect to this normal is given by the appropriate solution to

$$\cos\alpha_1 = \hat{e}_2 \cdot \hat{r}_{21} = \frac{2\cos\theta_2}{(3\cos^2\theta_2 + 1)^{1/2}} \ . \tag{2.10}$$

The solution to this equation gives the direction of the electric field uniquely, in terms of the orientation of the wall dipole at minus infinity (see Fig. 1).

The density profile $\rho_1(z, \mathbf{E}_2, \Omega_1)$ of dipolar molecules at a distance z from the wall depends on the dipole orientation Ω_1, on the direction of the electric field $\mathbf{E}_2$ and on other parameters of the system. It is obtained from the relation[1]

$$\rho_1(z, \mathbf{E}_2, \Omega_1) = \lim_{R_2 \to \infty} \left\{ \lim_{\rho 2 \to 0} \rho_1 \left[h_{21}(r_{21}, \Omega_2, \Omega_1) + 1 \right] \right\} \ , \tag{2.11}$$

where ρ_1 is the bulk density of species 1 and $h_{21}(r_{21}, \Omega_2, \Omega_1)$ is the total correlation function of species 1 and 2 in a binary mixture. The latter is the solution to the Ornstein–Zernike relation

$$h_{21} = c_{21} + \frac{1}{4\pi} \sum_{\gamma=1}^{2} \rho_\gamma h_{2\gamma} \bigcirc c_{\gamma 1} \ , \tag{2.12}$$

where $\bigcirc \equiv \int d\mathbf{r}_3 d\Omega_3$ is a convolution involving spatial and angular integrations. Assuming the invariant expansions

$$h_{21}(r_{21}, \Omega_2, \Omega_1) = h_{21}^s(r_{21}) + h_{21}^\Delta(r_{21})\,\Delta(2,1) + h_{21}^D(r_{21})\,D(2,1) \ , \tag{2.13}$$

$$c_{21}(r_{21}, \Omega_2, \Omega_1) = c_{21}^s(r_{21}) + c_{21}^\Delta(r_{21})\,\Delta(2,1) + c_{21}^D(r_{21})\,D(2,1) \ , \tag{2.14}$$

and using Wertheim's multiplication table[5] in Fourier space for the angular integrations, the Ornstein–Zernike relation reduces to three equations

$$h_{21}^s = c_{21}^s + \sum_{\gamma=1}^{2} \rho_\gamma h_{2\gamma}^s * c_{\gamma 1}^s \ , \tag{2.15}$$

$$\hat{h}_{21}^D = \hat{c}_{21}^D + \frac{1}{3}\sum_{\gamma=1}^{2} \rho_\gamma (\hat{h}_{2\gamma}^D * \hat{c}_{\gamma 1}^D + \hat{h}_{2\gamma}^D * c_{\gamma 1}^\Delta + h_{2\gamma}^\Delta * \hat{c}_{\gamma 1}^D) \ , \tag{2.16}$$

$$h_{21}^\Delta = c_{21}^\Delta + \frac{1}{3}\sum_{\gamma=1}^{2} \rho_\gamma (2\hat{h}_{2\gamma}^D * \hat{c}_{\gamma 1}^D + h_{2\gamma}^\Delta * c_{\gamma 1}^\Delta) \ , \tag{2.17}$$

when $* = \int d\mathbf{r}_3$ is a convolution involving only spatial integrations. In Eqs. (2.16) and (2.17)

$$\hat{h}_{\alpha\beta}^D(r) = h_{\alpha\beta}^D(r) - 3\int_r^\infty ds\, s^{-1} h_{\alpha\beta}^D(s) \tag{2.18}$$

and its inverse is

$$h_{\alpha\beta}^D(r) = \hat{h}_{\alpha\beta}^D(r) - \frac{3}{r^3}\int_0^r \hat{h}_{\alpha\beta}^D(s)\, s^2 ds \ , \tag{2.19}$$

with similar expressions for $\hat{c}_{\alpha\beta}^D(r)$ and $c_{\alpha\beta}^D(r)$ in which $\alpha, \beta = 1$ or 2. Inside the hard cores

$$\begin{aligned} &h_{\alpha\beta}^s(r) - 1 \ , \\ &h_{\alpha\beta}^D(r) = h_{\alpha\beta}^\Delta(r) = 0 \ , \quad r < R_{\alpha\beta} = R_\alpha + R_\beta \ , \end{aligned} \tag{2.20}$$

so that from Eq. (2.18)

$$\hat{h}_{\alpha\beta}^D(r) = -3K_{\alpha\beta} \ , \quad r < R_{\alpha\beta} \ , \tag{2.21}$$

where

$$K_{\alpha\beta} = \int_{R_{\alpha\beta}}^{\infty} h^D_{\alpha\beta}(s)\, s^{-1} ds \ . \tag{2.22}$$

Following Wertheim,[5] the relations for $\hat{h}^D_{21}(r)$ and $h^{\Delta}_{21}(r)$ may be uncoupled by taking linear combinations

$$h^{+}_{\alpha\beta}(r) = [\hat{h}^D_{\alpha\beta}(r) + \tfrac{1}{2} h^{\Delta}_{\alpha\beta}(r)]/3K_{\alpha\beta} \ , \tag{2.23}$$

$$h^{-}_{\alpha\beta}(r) = [\hat{h}^D_{\alpha\beta}(r) - h^{\Delta}_{\alpha\beta}(r)]/3K_{\alpha\beta} \ , \tag{2.24}$$

with analogous expressions for $c^{+}_{\alpha\beta}(r)$ and $c^{-}_{\alpha\beta}(r)$. The closure conditions (2.20) when applied to Eqs. (2.23) and (2.24) are equivalent to

$$h^{\pm}_{\alpha\beta}(r) = -1 \ , \quad r < R_{\alpha\beta} \ . \tag{2.25}$$

On using the linear combinations $h^{\pm}_{\alpha\beta}(r)$ in Eqs. (2.16) and (2.17), one finds

$$h^{\pm}_{21}(r) = c^{\pm}_{21}(r) + \sum_{\gamma=1}^{2} K_{\gamma\gamma}\, \rho^{\pm}_{\gamma}\, h^{\pm}_{2\gamma} * c^{\pm}_{\gamma 1} \ , \tag{2.26}$$

where $\rho^{+}_{\gamma} = 2\rho_{\gamma}$, $\rho^{-}_{\gamma} = -\rho_{\gamma}$. Equations (2.15) and (2.26) resemble the Ornstein–Zernike relations for a binary fluid, in which the molecular interactions are spherically symmetrical.

In the limit $R_2 \to \infty$, Eq. (2.19) together with Eqs. (2.23) and (2.24) yields

$$h^D_{21}(z) = [2h^{+}_{21}(z) + h^{-}_{21}(z) + 3]K_{21} \ . \tag{2.27}$$

As $\rho_2 \to 0$, Eqs. (2.15) and (2.26) reduce to

$$h^s_{21}(r) = c^s_{21}(r) + \rho_1\, h^s_{21} * c^s_{11} \tag{2.28}$$

and

$$h^{\pm}_{21}(r) = c^{\pm}_{21}(r) + K_{11}\rho^{\pm}_1 h^{\pm}_{21} * c^{\pm}_{11} \ , \tag{2.29}$$

which can be written in bipolar coordinates as

$$h^{\pm}_{21}(r) = c^{\pm}_{21}(r) + \frac{2\pi K_{11}\rho^{\pm}_1}{r} \int_0^{\infty} dt\, t\, h^{\pm}_{21}(t) \int_{|r-t|}^{r+t} ds\, s\, c^{\pm}_{11}(s) \ . \tag{2.30}$$

On substituting $r = R_2 + z$, $t = R_2 + y$ and on taking the wall limit $R_2 \to \infty$, we find, for $z > 0$,

$$h^{\pm}_{21}(z) = c^{\pm}_{21}(z) + 2K_{11}\pi\rho^{\pm}_1 \int_{-\infty}^{\infty} dy\, h^{\pm}_{21}(y) \int_{|z-y|}^{\infty} ds\, s\, c^{\pm}_{11}(s) \ , \tag{2.31}$$

where z is the distance of the center of the dipolar hard sphere from the wall. The integral between the limits $-\infty$ and ∞ may be simplified by noting that $h_{21}(y) = -1$, when $-\infty < y < 0$, and in addition $|z-y| = z - y$, when $z > 0$ and $-\infty < y < 0$. On changing the order of integration between $-\infty$ and 0,

$$\int_{-\infty}^{0} dy\, h^{\pm}_{21}(y) \int_{|z-y|}^{\infty} ds\, s\, c^{\pm}_{11}(s) = \int_{z}^{\infty} ds (z-s)\, s c^{\pm}_{11}(s) \ . \tag{2.32}$$

Defining the functions

$$B^{\pm}(z) = \int_0^z c^{\pm}_{11}(s)\, s\, ds \ , \quad D^{\pm}(z) = \int_0^z c^{\pm}_{11}(s)\, s^2 ds \ , \tag{2.33}$$

the wall–particle ± equations become

$$h^{\pm}_{21}(z) = c^{\pm}_{21}(z) + 2\pi K_{11}\rho^{\pm}_1 \{z\,[B^{\pm}(\infty) - B^{\pm}(z)] - [D^{\pm}(\infty) - D^{\pm}(z)]\} + 2\pi K_{11}\rho^{\pm}_1 \int_0^{\infty} dy\, h^{\pm}_{21}(y)\,[B^{\pm}(\infty) - B^{\pm}(|z-y|)] \ , \tag{2.34}$$

where the functions $B^{\pm}(z)$ and $D^{\pm}(z)$ are entirely determined by the interactions between the particles in the bulk fluid. An analogous equation can be written for the angularly independent part of the wall–particle total correlation function

$$h^s_{21}(z) = c^s_{21}(z) + 2\pi\rho_1 \Big\{ z\,[B^s(\infty) - B^s(z)] - [D^s(\infty) - D^s(z)] + \int_0^{\infty} dy\, h^s_{21}(y)\,[B^s(\infty) - B^s(|z-y|)] \Big\} \ , \tag{2.35}$$

where $B^s(z)$ and $D^s(z)$ have definitions which correspond exactly to $B^{\pm}(z)$ and $D^{\pm}(z)$.

In Eqs. (2.34) and (2.35), $\{c^s_{21}(z),\ c^s_{11}(s)\}$ and $\{c^{\pm}_{21}(z),\ c^{\pm}_{11}(s)\}$ are sets of two different, but consistent, direct correlation functions with corresponding closures (discussed in the next section) for the wall–particle and particle–particle interactions, respectively. The functions $c^s_{11}(r)$ and $c^{\pm}_{11}(r)$ for the bulk fluid particles are obtained in an independent calculation from

$$h^s_{11}(r) = c^s_{11}(r) + \rho_1\, h^s_{11} * c^s_{11} \ , \tag{2.36}$$

$$h^{\pm}_{11}(r) = c^{\pm}_{11}(r) + K_{11}\rho^{\pm}_1 h^{\pm}_{11} * c^{\pm}_{11} \ , \tag{2.37}$$

which are the one-component analogs of Eqs. (2.28) and (2.29) first derived in a seminal paper by Wertheim.[5] These equations carry their own closures for $h_{11}(r)(r < R_{11})$ and $c_{11}(r)(r > R_{11})$. We do not actually solve Eqs. (2.36) and (2.35) since nearly exact results are available from the work of Verlet and Weis[6] for hard spheres and from the study of Waisman, Henderson, and Lebowitz[7] for hard spheres against a wall. Our RLHNC approximation (Sec. III) implies that $h^s_{21}(z)$ is the exact wall–particle total correlation function for hard spheres against a hard wall. Equation (2.37) has been solved by Wertheim, in the mean spherical approximation,[6] while Patey and his colleagues have treated it in the LHNC and QHNC approximations,[8] using the Verlet–Weis theory for the hard-sphere interactions. We are therefore left with the necessity of solving only Eq. (2.34) under the appropriate closures for the wall–particle and particle–particle direction correlation functions.

The constants K_{11} and K_{21} determine the dipole moment m_1 and the electric field E_2 through the relations

$$\frac{4\pi m_1^2 \rho_1}{3kT} = Q_{+}(2K_{11}\rho_1 R_{11}^3) - Q_{-}(-K_{11}\rho_1 R_{11}^3) \tag{2.38}$$

and

$$\frac{m_1 E_0}{kT} = K_{21}\,[2Q_{+}(2K_{11}\rho_1 R_{11}^3) + Q_{-}(-K_{11}\rho_1 R_{11}^3)] \ , \tag{2.39}$$

where k and T are the Boltzmann constant and absolute temperature, respectively, and $Q_{+-}(\rho_1 R_{11}^3)$ is defined by:

$$Q_{+-}(\rho_1 R_{11}^3) = 1 - 4\pi\rho_1 \int_0^{\infty} c^{+}_{11}(r,\ \rho_1)\, r^2 dr \ . \tag{2.40}$$

Equation (2.38) has been derived by Wertheim[5] in the mean spherical approximation, but its extension to the LHNC (or RLHNC) approximation is straightforward; nevertheless we present it for completeness and as a prelude to the derivation of (2.39), which Isbister and Freasier[1] discussed in the mean spherical approximation. The derivation of Eq. (2.38) rests on the asymptotic form of $c^D_{11}(r)$ [see Eqs. (3.1) and (3.6)]

$$c_{11}^D(r) \to \frac{\beta m_1^2}{r^3} D(2,1) \ , \quad \text{as } r \to \infty \ . \tag{2.41}$$

On inserting this in

$$\hat{c}_{11}^D(r) = c_{11}^D(r) - 3\int_r^\infty ds\, s^{-1} c_{11}^D(s) \ , \tag{2.42}$$

one sees that $\hat{c}_{11}^D(r)$ is short ranged and tends to zero as $r \to \infty$:

$$\hat{c}_{11}^D(r) \to 0 \ , \quad \text{as } r \to \infty \ . \tag{2.43}$$

When the inverse relation [cf. Eqs. (2.19) and (2.18)]

$$c_{11}^D(r) = \hat{c}_{11}^D(r) - \frac{3}{r^3}\int_0^r \hat{c}_{11}(s)\, s^2 ds \tag{2.44}$$

is taken to the limit $r \to \infty$, one also finds that

$$\frac{m_1^2}{kT} = -3\int_0^\infty \hat{c}_{11}^D(s)\, s^2 ds$$

$$= -3K_{11}\int_0^\infty [2c_{11}^+(s, 2K_{11}\rho_1) + c_{11}^-(s, -K_{11}\rho_1)]\, s^2 ds \ , \tag{2.45}$$

where we have used the analogs of Eqs. (2.23) and (2.24) applied to $\hat{c}_{11}^D(s)$ in the last step. The result given in Eq. (2.38) follows immediately on applying Eq. (2.40).

The relation between K_{21} and E_0 is also derived from the asymptotic from of $c_{21}^D(r)$ in the MS and LHNC approximations [see Eqs. (3.1) and (3.6) in Sec. III]. The equation for dipolar mixtures which corresponds to Eq. (2.45) is[9]

$$\lim_{r_{21}\to\infty} \frac{m_2 m_1}{r_{21}^3 kT} = -\lim_{r_{21}\to\infty} \frac{3K_{21}}{r_{21}^3}\int_0^{r_{21}} [2c_{21}^+(s) + c_{21}^-(s)]\, s^2 ds \ , \tag{2.46}$$

where we have not canceled the r_{21}^3 in the denominator, because we intend to take the wall limit. Substituting $r_{21} = R_2 + z$, and taking the limit $R_2 \to \infty$, reduces the left hand side of Eq. (2.46) to $m_1 E_0/kT$, and replaces the upper limit of the integral in Eq. (2.46) by ∞. The Fourier transform of Eq. (2.29), which is an Ornstein–Zernike equation for mixtures, as $\rho_2 \to 0$, yields

$$\tilde{c}_{21}^{\pm}(k) = [1 - K_{11}\rho_1^{\pm}\tilde{c}_{11}^{\pm}(k)]\,\tilde{h}_{21}^{\pm}(k) \ , \tag{2.47}$$

from which, when $k = 0$, we have

$$\int_0^\infty c_{21}^{\pm}(s)\, s^2 ds = [1 - K_{11}\rho_1^{\pm}\tilde{c}_{11}^{\pm}(0)]\int_0^\infty h_{21}^{\pm}(s)\, s^2 ds \ . \tag{2.48}$$

In the above, the "~" represents the three dimensional Fourier transform

$$\tilde{t}(k) = \int d\mathbf{r} \exp(i\mathbf{k}\cdot\mathbf{r})\, t(|\mathbf{r}|) \ ,$$

and $t \equiv c$ or h.

Since $h_{21}^{\pm}(s)$ is a short-ranged function equal to -1 for $s < R_{21}$, it readily follows that

$$\lim_{R_2\to\infty} \frac{1}{r_{21}^3}\int_0^\infty h_{21}^{\pm}(s)\, s^2 ds = -\tfrac{1}{3} \ . \tag{2.49}$$

Hence,

$$\frac{m_1 E_0}{kT} = K_{21}[2[1 - K_{11}\rho_1^+\tilde{c}_{11}^+(0)] + [1 - K_{11}\rho_1^-\tilde{c}_{11}^-(0)]] \ , \tag{2.50}$$

which is identical to Eq. (2.39). It should be emphasized that Eqs. (2.38) and (2.39) are relations derived from the asymptotic forms of c_{11}^D and c_{21}^D in the MS and LHNC approximations. The dipole moment m_1 and the electric field E_2 are determined from K_{11} and K_{21}, after the solutions to Eq. (2.37) have been obtained.

The constant K_{21} also retrieves the coefficients $h_{21}^D(z)$ and $h_{21}^\Delta(z)$, which appear in the invariant expansion of the wall–particle correlation functions

$$h_{21}(z, \mathbf{E}_2, \Omega_1) = h_{21}^s(z) + h_{21}^D(z)\, D(2,1) + h_{21}^\Delta(z)\, \Delta(2,1) \tag{2.51}$$

by inverting Eq. (2.23) and (2.24) and using Eq. (2.27). Both $h_{21}^s(z)$ (for the closure rules considered in the next section) and $h_{21}^\Delta(z)$ are short-ranged functions and tend to zero as $z \to \infty$, and the asymptotic form of $h_{21}^D(z)$ is therefore

$$\lim_{z\to\infty} h_{21}^D(z) = 3K_{21} \ , \tag{2.52}$$

which follows from Eq. (2.27) and the fact that $h_{21}^{\pm}(z)$ is also short ranged. The asymptotic form of the wall–particle correlation function for the RLHNC closure, discussed in the next section, coincides with that of the MS approximation[1] and is therefore given by

$$\lim_{z\to\infty} h_{21}(z, \mathbf{E}_2, \Omega_1) = 3K_{21} D(2,1) \tag{2.53}$$

$$= \frac{3m_1 E_0 D(2,1)}{kT\,[2Q(2K_{11}\rho_1 R_{11}^3) + Q(-K_{11}\rho_1 R_{11}^3)]} \tag{2.54}$$

$$= \frac{[3E_0^* D(2,1)]}{T^*\,[2Q(2K_{11}\rho_1 R_{11}^3) + Q(-K_{11}\rho_1 R_{11}^3)]} \ , \tag{2.55}$$

where

$$T^* = \left(\frac{kTR_{11}^3}{m_1^2}\right) \tag{2.56}$$

and

$$E_0^* = \frac{E_0 R_{11}^3}{m_1} = \frac{|\mathbf{E}_2|}{(3\cos^2\theta_2 + 1)^{1/2}}\,\frac{R_{11}^3}{m_1} \ . \tag{2.57}$$

Since the electric field is independent of the distance from the wall, $h_{21}(z, \mathbf{E}_2, \Omega_1)$ does not decrease to zero as $z \to \infty$, unless the magnitude of the electric field or $D(2,1)$ is also zero. The angular average of $h_{21}(z, \mathbf{E}_2, \Omega_1)$ is however zero in the limit $z \to \infty$:

$$\lim_{z\to\infty} \int h_{21}(z, \mathbf{E}_2, \Omega_1)\, d\Omega_1 = 0 \tag{2.58}$$

since the angular averages of $D(2,1)$ and $\Delta(2,1)$ are zero and

$$\lim_{z\to\infty} h_{21}^s(z) = 0 \ . \tag{2.59}$$

We shall now consider the details of these equations in the context of the mean spherical and linearized hypernetted chain closure rules.

III. THE CLOSURE RELATIONS

The closures for the wall–particle direct correlation functions are readily derived by taking the wall limit of the corresponding closures in the bulk fluid.

A. MSA

The closure for the direct correlation function is

$$c_{\alpha\beta}(r) = \frac{m_\alpha m_\beta}{kT\, r^3} D(1,2) \ , \quad \text{for } r > R_{\alpha\beta} \ , \tag{3.1}$$

which is equivalent to

$$c^{\pm}_{\alpha\beta}(r) = 0 \ , \quad \text{for } r > R_{\alpha\beta} \ . \tag{3.2}$$

This is unaffected, for $z > R_{21}$, on taking the wall limit of $c^{\pm}_{21}(r)$.

B. LHNC approximation

Starting with the hypernetted chain (HNC) approximation

$$c_{\alpha\beta}(2,1) = h_{\alpha\beta}(2,1) - \ln g_{\alpha\beta}(2,1) - V_{\alpha\beta}(2,1)/kT \quad (r > R_{\alpha\beta}) \tag{3.3}$$

and using the invariant expansions of $c_{\alpha\beta}(2,1)$ and $h_{\alpha\beta}(2,1)$ [cf. Eqs. (2.13) and (2.14)], one finds

$$c_{\alpha\beta}(r) = h^s_{\alpha\beta}(r) - \ln\left\{ g^s_{\alpha\beta} \frac{[1 + h^D_{\alpha\beta}(r) D(2,1) + h^{\Delta}_{\alpha\beta} \Delta(2,1)]}{g^s_{\alpha\beta}(r)} \right\} - \frac{V^s_{\alpha\beta}(r)}{kT} + \frac{m_\alpha m_\beta}{kT\, r^3} D(2,1) \ , \tag{3.4}$$

where $V^s_{\alpha\beta}$ is the spherically symmetric part of the potential. Expanding the logarithm up to the linear term, and collecting and comparing coefficients of 1, $D(2,1)$, and $\Delta(2,1)$, we have

$$c^s_{\alpha\beta}(r) = h^s_{\alpha\beta}(r) - \ln g^s_{\alpha\beta}(r) - V^s_{\alpha\beta}(r)/kT \ , \tag{3.5}$$

$$c^D_{\alpha\beta}(r) = h^D_{\alpha\beta}(r)\,[1 - g^s_{\alpha\beta}(r)^{-1}] + \frac{m_\alpha m_\beta}{r^3 kT} \ , \tag{3.6}$$

$$c^{\Delta}_{\alpha\beta}(r) = h^{\Delta}_{\alpha\beta}(r)\,[1 - g^s_{\alpha\beta}(r)^{-1}] \ . \tag{3.7}$$

Defining

$$b^D_{\alpha\beta}(r) = h^D_{\alpha\beta}(r)\,[1 - g^s_{\alpha\beta}(r)^{-1}] \ , \tag{3.8}$$

$$b^{\Delta}_{\alpha\beta}(r) = h^{\Delta}_{\alpha\beta}(r)\,[1 - g^s_{\alpha\beta}(r)^{-1}] \ , \tag{3.9}$$

with $\hat{b}^D_{\alpha\beta}(r)$ and $b^{\pm}_{\alpha\beta}(r)$ also defined by equations analogous to Eqs. (2.18), (2.23), and (2.24), respectively, the last two equations can be written in the form

$$c^{\pm}_{\alpha\beta}(r) = b^{\pm}_{\alpha\beta}(r) \ , \quad r > R_{\alpha\beta} \ . \tag{3.10}$$

In the RLHNC, Eq. (3.5) is replaced by the exact closure for hard spheres against a wall.

In the wall limit, $\hat{b}^D_{21}(z) = b^D_{21}(z)$, and making use of Eq. (2.27), the closure condition for the wall–particle direct correlation function becomes

$$c^{\pm}_{21}(z) = [1 + h^{\pm}_{21}(z)]\,[1 - g^s_{21}(z)^{-1}] \ , \quad z > 0 \ . \tag{3.11}$$

On substituting this in Eq. (2.34), we have, for $z > 0$,

$$h^{\pm}_{21}(z) = [g^s_{21}(z) - 1] + g^s_{21}(z)\, 2\pi K_{11} \rho^{\pm}_1 \left\{ z\,[B^{\pm}(\infty) - B^{\pm}(z)] + [D^{\pm}(\infty) - D^{\pm}(z)] + \int_0^{\infty} h^{\pm}_{21}(z)\,[B^{\pm}(\infty) - B^{\pm}(|z - y|)]\, dy \right\} . \tag{3.12}$$

When $g^s_{21}(z) = 1$, the formal equation for $h^{\pm}_{21}(z)$ in the MSA approximation is recovered.

The above equations (3.12) were solved iteratively on a computer to generate the accompanying figures.

IV. RESULTS AND DISCUSSION

The solution of Eq. (2.51), for $h_{21}(z, \mathbf{E}_2, \Omega_1)$, was obtained as the confluence of three distinct computations:

(1) The bulk correlation functions were calculated in the manner described by Patey, from Eq. (2.37). The reduced dipole moment dependence of this relation contained in the constant K_{11}, through Eq. (2.38), may also be expressed in the MSA and RLHNC approximations as

$$m^{*2}_1 \equiv \frac{m^2_1}{kT\, R^3_{11}} = c^D_{11}(R^+_{11}) - b^D_{11}(R^+_{11}) \ , \tag{4.1}$$

where $c^D_{11}(R^+_{11})$ and $b^D_{11}(R^+_{11})$ are the values of $c^D_{11}(r)$ and $b^D_{11}(r)$ immediately outside contact. The value of K_{11} was adjusted until this difference assumed the desired reduced dipole moment. The iteration of Eq. (2.37) was performed using fast Fourier transform techniques and mixed solutions to speed convergence. The bulk fluid correlation functions obtained showed excellent agreement with those of Patey.[8]

(2) The electric field which emerges from the wall was determined by Eqs. (2.9), (2.39), and (2.40). The field angle α_1 of Fig. 1 was taken, in separate calculations, as 0°, 45°, and 90°. The field angle is related to the wall–dipole orientation θ_2 through Eq. (2.10), the solution of which appears in Fig. 1. The magnitude of the reduced electric field

$$|E^*_2| = \frac{|\mathbf{E}_2| R^3_{11}}{m_1} = \frac{E_0 (3\cos^2\theta_2 + 1)^{1/2} R^3_{11}}{m_1} \tag{4.2}$$

was taken, as in the earlier work of Isbister and Freasier, to be 8/3, with the reduced dipole moment squared m^{*2}_1 fixed at either 0.5 or 1.0. For purposes of comparison of these parameters to a molecular system, the reduced dipole moment squared for HCl (m_1 = 1.03 D) at 275 °K, assuming a diameter of 3.5 Å, is approximately 0.65. A reduced field strength of 8/3 for this system corresponds to an electric field of nearly 1.9×10^9 V/m or a surface charge density σ of 1 electronic charge/1000 Å^2.

We have also carried out calculations at the same surface charge density (or electric field E_2) for a fluid at a reduced density of 0.7 with the reduced dipole moment $m^*_1 = 2.0$. These numbers correspond approximately to those appropriate for liquid water ($m_1 = 1.85$ D, $R_{11} = 2.76$ Å) at room temperature. The reduced electric field E^*_2 [which contains m_1 and R^3_{11} in its definition (4.2)] is now only 0.71. (It may be useful for the reader to bear in mind that it is an artifact of our definition of E^*_2 that an increase in the dipole moment m_1 results either in a reduction of E^*_2 when the surface charge density is held constant, or an increase in the surface charge density when E^*_2 is unchanged.)

(3) The spherically symmetric part of Eq. (2.51), i.e., $h^s_{21}(z)$, was determined using the technique of Waisman, Henderson, and Lebowitz.[7] The function $h^s_{21}(z)$ was first obtained from Eq. (2.28) as the Percus–Yevick solution and then corrected to produce an essen-

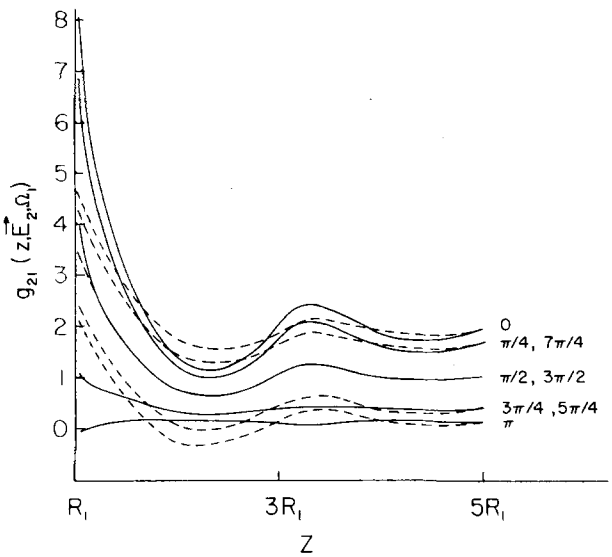

FIG. 2. The wall–particle distribution functions $g_{21}(z, \mathbf{E}_2, \Omega_1)$ as a function of the distance z from the wall for different orientations Ω_1 of the fluid dipoles where $E_2^* = 8/3$, $m_1^{*2} = 0.5$, $\rho_1^* = 0.573$, and $\alpha_1 = 0°$. R_1 is the radius of a fluid dipole. —— RLHNC approximation, ----- MS approximation.

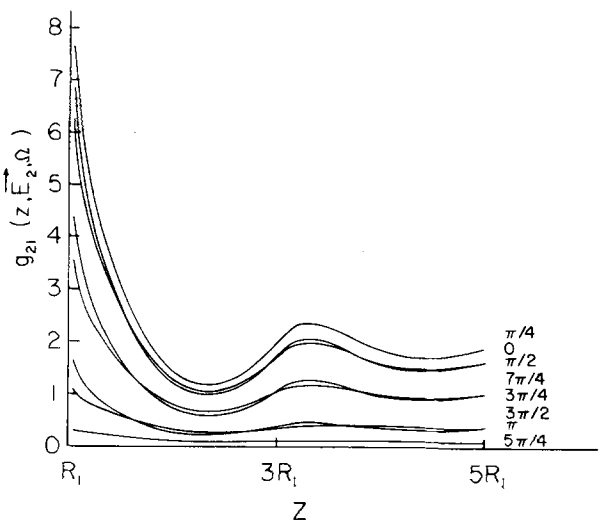

FIG. 3. Wall–particle distribution functions for the system depicted in Fig. 2 except that $\alpha_1 = 45°$.

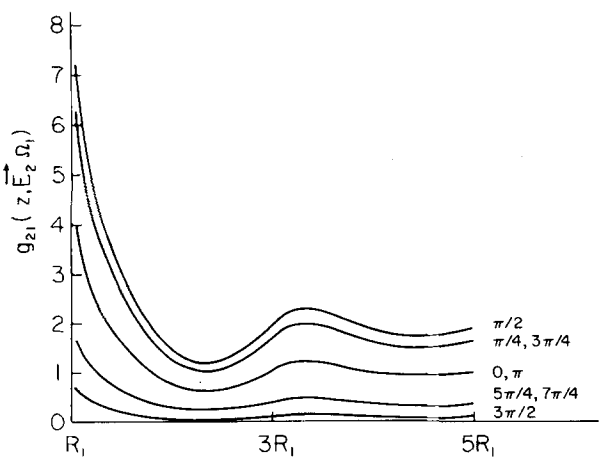

FIG. 4. Wall–particle distribution functions for the systems depicted in Figs. 2 and 3 except that $\alpha_1 = 90°$.

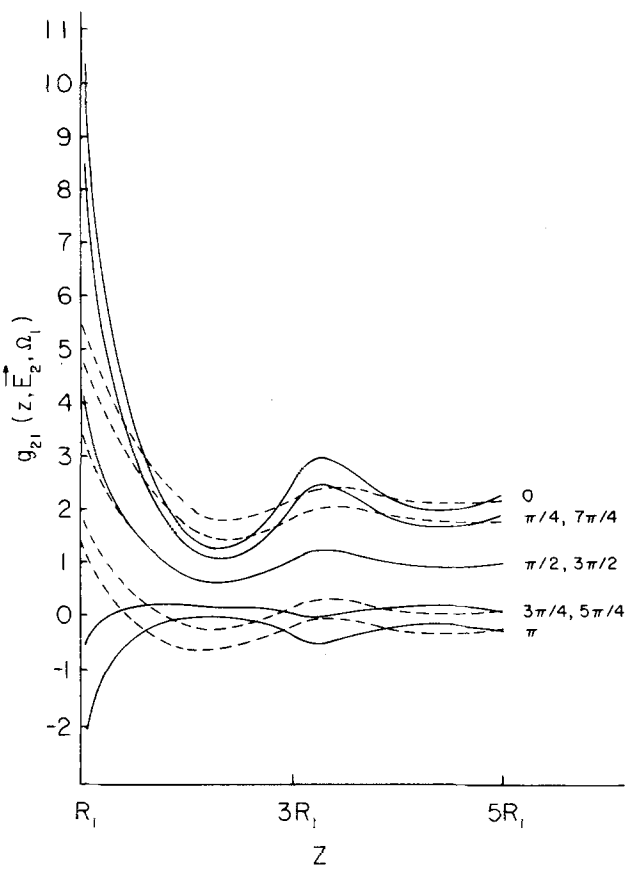

FIG. 5. The wall–particle distribution function $g_{21}(z, \mathbf{E}_2, \Omega_1)$ for the system depicted in Fig. 1 except that $m_1^{*2} = 1.0$.

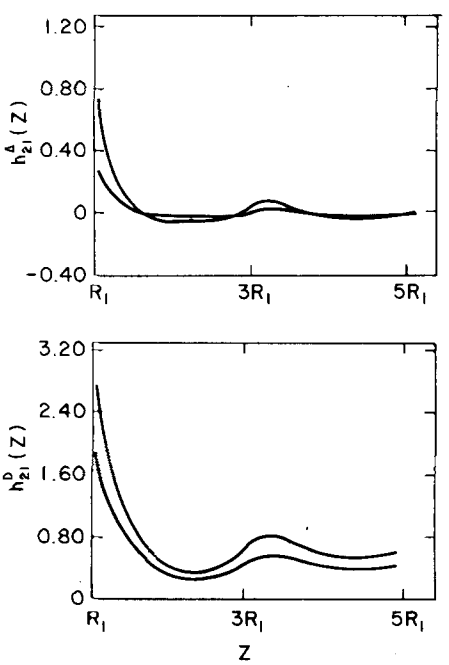

FIG. 6. The expansion coefficients $h_{21}^A(z)$ and $h_{21}^D(z)$ as a function of the wall–particle distance z when $E_2^* = 8/3$ and $\rho_1^* = 0.573$. The upper and lower curves, in each case, are for $m_1^{*2} = 1.0$ and 0.5, respectively.

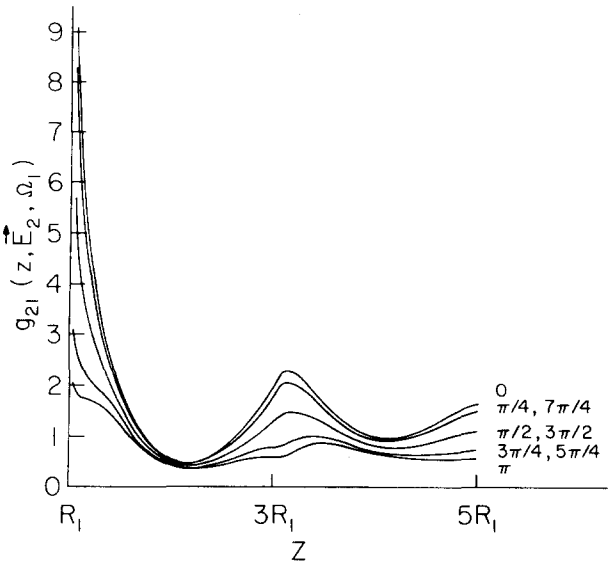

FIG. 7. The wall–particle distribution function $g_{21}(z, \mathbf{E}_2, \Omega_1)$ as a function of the distance z from the wall, for different orientations Ω_1 of the fluid dipoles when $E_2^* = 0.71$, $m_1^{*2} = 4.0$, $\rho_1^* = 0.7$, and $\alpha_1 = 0$. The reduced parameters m_1^* and ρ_1^* are those appropriate for liquid water at room temperature ($m_1 = 1.85$ D, $R_{11} = 2.76$ Å). The reduced electric field $E_2^* = 0.71$ corresponds to a surface density of 1 electronic charge/1000 Å^2.

tially exact wall–particle correlation function in comparison to Monte Carlo simulation. The reduced density of hard spheres, upon which $h_{21}^s(z)$ depends solely, was taken as $\rho^* = \rho_1 R_{11}^3 = 0.573$.

The computations were combined through Eqs. (2.23), (2.24), and (3.12) to yield the coefficients of the angular functions of Eq. (2.51). The integrals over bulk correlation functions (2.33) as well as the integral of Eq. (3.12) were performed by trapezoidal approximation. The iterative solution to Eq. (3.12) was rapidly convergent. Finally, the expansion coefficients were inserted into Eq. (2.51).

In Figs. 2–5 we present our results for $g_{21}(z, \mathbf{E}_2, \Omega_1)$ in the RLHNC approximation. The expansion coefficients $h_{21}^D(r)$ and $h_{21}^\Delta(r)$ are shown in Fig. 6. A comparison of RLHNC and MSA results, for a field angle of zero and reduced dipole moment squared of 0.5 and 1.0, are shown in Figs. 2 and 5, respectively.

In the case of $m_1^{*2} = 0.5$, $E_2^* = 8/3$, and $\rho_1^* = 0.573$ $g_{21}(z, \mathbf{E}_2, \Omega_1)$ in the RLHNC approximation assumes negative values only very near and at contact for a dipole orientation in opposition to the field. For higher values of $m_1^{*2} = 1.0$, at the same reduced electric field and fluid density, these regions are more pronounced and extended in range (Fig. 5). An increase in m_1^{*2} from 0.5 to 1.0 at constant E_2^* and ρ_1^*, however, corresponds to a fourfold increase in the surface charge density from 1 electronic charge/1000 Å^2 to one every 250 Å^2. Both the RLHNC and MSA treatments result in distributions showing exhanced adsorption for favorable dipole orientations, but the repulsive interactions of the electric field with unfavorably aligned dipoles is more clearly visible in the RLHNC approximation. This theory, like the MSA, is essentially linear in character, and cannot prevent the distribution functions from becoming negative when the dipoles are aligned against the field, if at the same time the theory predicts a large enhancement of the adsorption of dipoles aligned with the field. When, for example, the electric field is perpendicular to the wall, both theories predict that the density profiles (see Figs. 2 and 5) are symmetrical about the profile for dipoles perpendicular to the field ($\theta_1 = \pi/2$ or $3\pi/2$). A large enhancement of dipoles aligned with the field would lead to an equally large depletion of dipoles oriented against the field, which may require negative wall–particle distribution functions. Further improvements beyond the RLHNC approximation would then be necessary. Figure 7 shows, however, that the RLHNC theory provides plausible density profiles even when the square of the dipole moment m_1^{*2} is increased to 4.0 but the surface charge density is maintained at 1 electronic charge/1000 Å^2.

ACKNOWLEDGMENTS

Support from the National Science Foundation, Contract No. CHE 77-10023, and from the Office of Naval Research, Contract No. N00014 78-c-0724 are gratefully acknowledged. One of us (D.I.) would like to thank the University of New South Wales for a leave of absence, and the Australian Research Grants Commission for its assistance.

[1] D. J. Isbister and B. C. Freasier, J. Stat. Phys. 20, 331 (1979). The notation that is used in this paper is slightly different. In particular, R_α is the radius of the α species rather than the diameter, and E_2 and E_0 as defined here are E_0 and E_0/f, respectively, of Isbister and Freasier.
[2] The LHNC approximation for dipolar fluids proposed by G. N. Patey [Mol. Phys. 34, 427 (1977)] is identical to the single superchain approximation suggested earlier by M. S. Wertheim [Mol. Phys. 26, 1425 (1973)]. The analog of this approximation for the wall–particle closure is used in this study.
[3] G. Stell and J. J. Weis, Phys. Rev. A 21, 645 (1980).
[4] E. Helfand, H. Reiss, H. L. Frisch, and J. L. Lebowitz, J. Chem. Phys. 33, 1379 (1960); see also J. W. Perram and E. R. Smith, Proc. R. Soc. (London) Ser. A 353, 193 (1977).
[5] M. S. Wertheim, J. Chem. Phys. 55, 4291 (1971).
[6] L. Verlet and J. J. Weis, Phys. Rev. A 5, 939 (1972).
[7] E. Waisman, D. Henderson, and J. L. Lebowitz, Mol. Phys. 32, 1373 (1976).
[8] G. N. Patey, Mol. Phys. 34, 427 (1977); G. N. Patey, D. Levesque, and J. J. Weis, Mol. Phys. 38, 1635 (1979).
[9] (a) D. Isbister and R. J. Bearman, Mol. Phys. 28, 1297 (1974); 32, 597 (1976); (b) D. Isbister, Mol. Phys. 32, 949 (1976).